EFFECT OF HEAT TREATMENT ON MICROSTRUCTURE AND MECHANICAL PROPERTIES OF ALLOY Mg – 10% Gd – 3% Y – 0.6% Zr

Zhi-bing Ding,[1] Ruo-peng Lu,[1] Hua Hou,[1] Jin-zhong Tian,[1] and Yu-hong Zhao[1]

The microstructure, mechanical properties and fracture behavior of magnesium alloy Mg – 10% Gd – 3% Y – 0.6% Zr is studied in cast condition and after T4 and T6 treatments. It is shown that in cast condition the alloy contains an α-phase (a magnesium-base solid solution) and a $Mg_{24}(Gd, Y)_5$ eutectic phase. After the solution treatment the eutectic phase dissolves in the α-matrix containing cuboid particles of a phase enriched with gadolinium and yttrium. The hardness and the tensile strength criteria are used to determine the optimum treatment for the cast alloy, i.e., 8-h solution treatment at 500°C and 16-h aging at 220°C (T6). This mode of heat treatment provides the best mechanical properties.

Key words: magnesium alloys, heat treatment, microstructure, mechanical properties, fracture.

INTRODUCTION

The low density, high specific strength and high machinability of magnesium alloys make them promising materials for the aerospace, automotive, military, and biomedical industries [1 – 4]. The automotive industry employs commercial magnesium alloys AZ91D (Mg – 9% Al – 0.7% Zn),[2] AM50 (Mg – 5% Al – 0.4% Mn) and AM60B (Mg – 6% Al – 0.4% Mn). These alloys possess a very good combination of mechanical properties, corrosion resistance and die castability [5]. However, they soften above 125°C and become inapplicable at these temperatures [6]. It has been reported that introduction of rare-earth metals (REM) into magnesium alloys elevates their strength at room and elevated temperatures as well as the creep resistance [7, 8]. The Mg – Gd – Y – Zr system is the most promising for rapid hardening under aging and exhibits good thermal stability of the main hardening phase up to 250°C [9]. Alloys of the Mg – Gd and Mg – Gd – Y systems are strengthened much even due to aging above 200°C due to precipitation of a β''-phase with structure $D0_{19}$ and a β'-phase with body-centered orthorhombic structure [10].

The Gd, Y and Zr elements in the Mg – Gd – Y – Zr system affect considerably the microstructure and mechanical properties of the alloys [11, 12]. It has been reported in [9]

that the process of decomposition of the supersaturated solid solution in alloy Mg – 10Gd – 3Y – 0.4Zr at 250°C occurs in four stages, i.e., Mg-base supersaturated α-solid solution (S.S.S.S.) $\rightarrow$ metastable $\beta''(D0_{19})$-phase $\rightarrow$ metastable β'-phase (orthorhombic body-centered) $\rightarrow$ metastable β_1-phase (fcc) $\rightarrow$ stable β-phase (fcc). According to the data of [13], the metastable β'-phase is the main hardening phase responsible for the maximum hardness of alloys of the Mg – Gd – Y – Zr system.

Several studies have been devoted to the relation between microstructure and mechanical properties of alloys of the Mg – Gd – Y – Zr system [14 – 16]. A Mg – Gd – Y – Zr alloy with concentration ratio $x(Gd)/x(Y) \approx 10/3$ has high mechanical properties in cast and heat-treated conditions [13]. For this reason, we chose alloy Mg – 10Gd – 3Y – 0.6Zr as the object of the present study. The aim of the work was to optimize the process of heat treatment of alloy Mg – 10Gd – 3Y – 0.6Zr and to study its microstructure, mechanical properties and fracture behavior.

METHODS OF STUDY

We melted Mg – 30% Gd, Mg – 30% Y, Mg – 30% Zr master alloys and pure magnesium in an induction furnace to obtain a Mg – 10Gd – 3Y – 0.6Zr alloy. The melting was conducted in a crucible from a low-carbon steel at 780°C at a medium frequency in an argon atmosphere. After adequate stirring, the melt was cooled in water. The homogenizing treatment (for solid solution, T4) was conducted at a tempe-

---

[1] College of Materials Science and Engineering, North University of China, Taiyuan, China (e-mail: houhua@263.net).

[2] Here and below in the paper the content of the elements is given in weight percent.
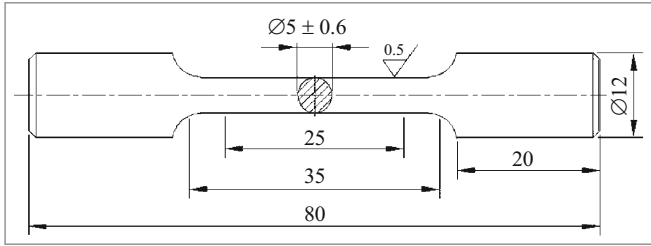
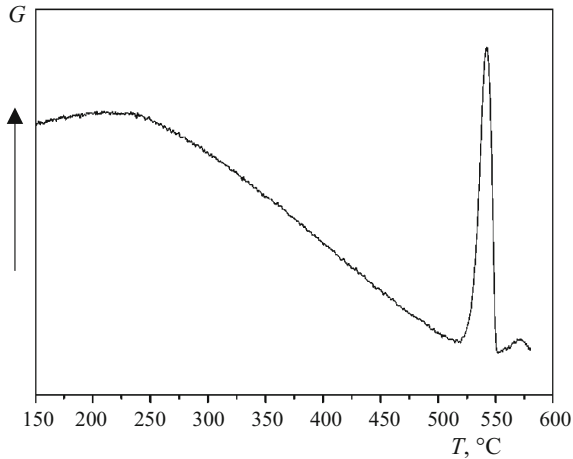**Fig. 1.** Shape and sizes of a specimen for tensile testing.

Fig. 2. DSC curves for cast Mg – 10Gd – 3Y – 0.6Zr (G is the heat flux).

rature of from 480 to 520°C for 5 – 8 h, after which the samples were quenched in water. After the solution treatment, the alloy was subjected to aging in air at 200°C (T6).

The specimens for optical (OM) and scanning electron microscopy (SEM) were prepared by the standard method by grinding against a SiC abrasive paper and polishing in a MgO suspension. The etching was conducted in a 4% solution of nital. The phase analysis was performed using a Rigaku D/MAX2500PC diffractometer in copper radiation at a scanning speed of 15 °/min in an angle range from 20 to 90°. The mean grain size d was determined by the mean linear intercept technique (ASTM E112–96) counting at least 300 grain boundaries for each specimen. The differential scanning calorimetry (DSC) was performed with the use of a NETZSCH STA 44TC device in the temperature range of 150 – 580°C at heating and cooling rates of 15 K/min.

The Vickers hardness was measured at a load of 19.6 N with 15-sec exposure; each value was averaged after at least 10 measurements. The tensile tests were performed for standard cylindrical specimens (Fig. 1) using a Zwick/Roell Z020 testing machine at a crosshead speed of 1.5 mm/min. The values were averaged after three measurements. The fracture surfaces were studied under a scanning electron microscope.

RESULTS AND DISCUSSION

Figure 2 presents the DSC curves for the cast alloy. The temperature of the peak of the endothermic reaction of dissolution of the eutectic phase was 542.2°C. Therefore, the homogenizing was conducted at 480, 500 and 520°C.

Figure 3 presents the microstructure of the alloy and the results of the energy dispersive chemical analysis at points A and B. It can be seen that the grains of the α-phase are surrounded by a net of eutectic phases. By the data of the local
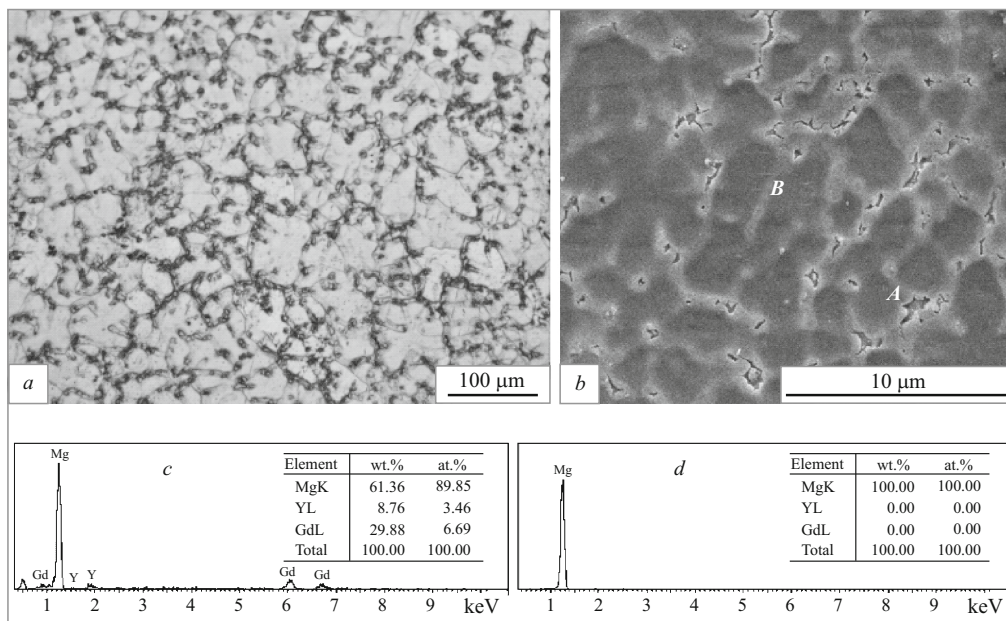

Fig. 3. Optical (a) and scanning electron microscopy (b) of cast Mg – 10Gd – 3Y – 0.6Zr and EDS results for points A (c) and B (d).
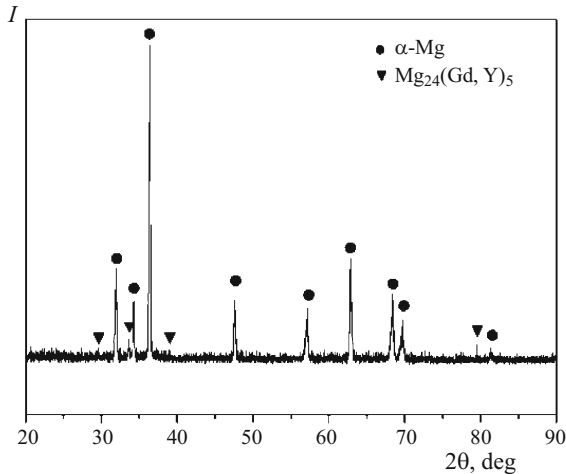
Fig. 4. X-ray diffraction pattern of alloy Mg – 10Gd – 3Y – 0.6Zr in cast condition.

x-ray diffraction chemical analysis (Fig. 4) the structure of the cast magnesium alloy Mg – 10Gd – 3Y – 0.6Zr is represented by a magnesium-base α-solid solution and a $Mg_{24}(Gd, Y)_5$ phase.

Figure 5 presents the microstructure (OM) of the alloy after solution treatment at different temperatures and dura-

tions of the hold. It can be seen that prolongation of the hold at a constant temperature results in grain growth. It is also obvious that increase in the hold is accompanied by preferred growth of some grains, while the other grains virtually preserve their size. Fine particles of a eutectic phase are preserved over grain boundaries after a 2-h hold.

The rate of grain growth at 520°C is higher than at 480°C, which can be seen from Fig. 6. In the cast condition, the grain size is 31 μm. The maximum grain size (96.7 μm) is observed after the 8-h treatment at 520°C. After the T6 treatment (aging) the grain size remains virtually invariable as compared to the specimens treated for solid solution.

The properties of the alloy after different modes of solution treatment are presented in Table 1. It can be seen that the elongation increases and the yield strength and the ultimate strength decrease somewhat as compared to the cast condition. This is explainable by dissolution of the eutectic phase in the matrix under the solution treatment. There is a tendency to increase in the elongation and in the ultimate strength with growth of the temperature of the solution treatment (the elongation increases to 10.6% after a 5-h treatment at 520°C). This is also connected with dissolution of the eutectic phase.
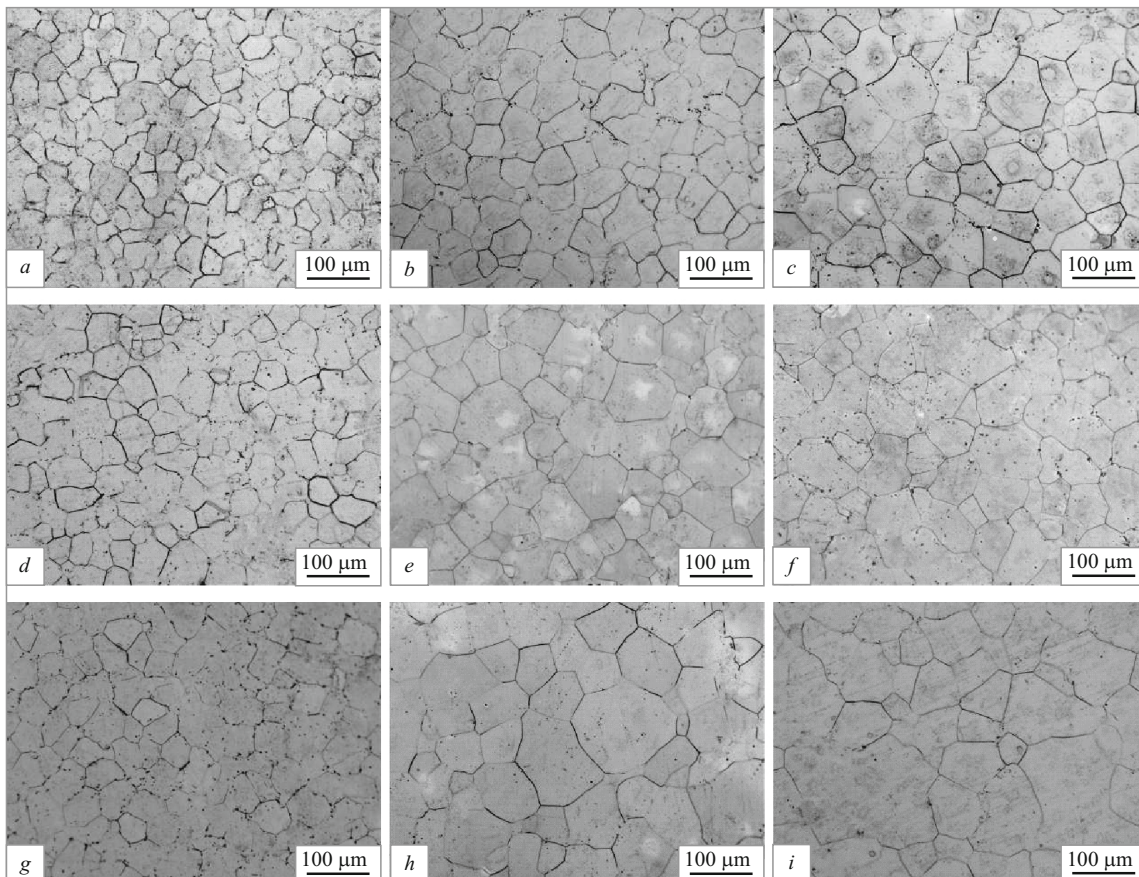

Fig. 5. Microstructure (OM) of alloy Mg – 10Gd – 3Y – 0.6Zr after casting and T4 treatment: *a*) 480 8C, 2 h; *b*) 480°C, 5 h; *c*) 480°C, 8 h; *d*) 500°C, 2 h; *e*) 500°C, 5 h; *f*) 500°C, 8 h; *g*) 520°C, 2 h; *h*) 520°C, 5 h; *i*) 520°C, 8 h.
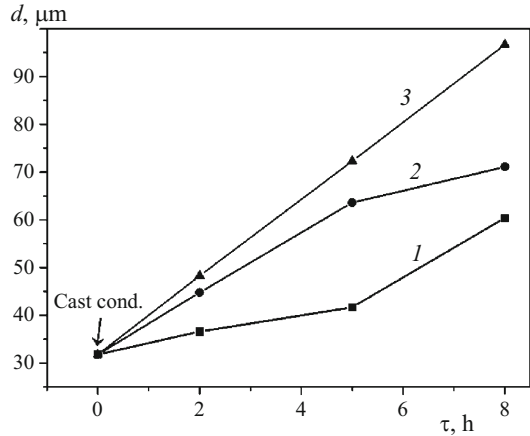
Fig. 6. Grain size (d) of alloy Mg − 10Gd − 3Y − 0.6Zr as a function of the duration of treatment for solid solution at different temperatures: *1*) 480°C; *2*) 500°C; *3*) 520°C.

TABLE 1. Mechanical Properties of Alloy Mg − 10Gd − 3Y − 0.6Zr (Tensile Tests) after Different Solution Treatments

Treatment mode T4	$\sigma_{0.2}$, MPa	σ_r, MPa	δ, %
Cast condition	186	226	7.3
480°C, 5 h	162	217	8.2
480°C, 8 h	180	225	9.4
500°C, 5 h	168	219	8.4
500°C, 8 h	166	223	10.1
520°C, 5 h	172	223	10.6
520°C, 8 h	183	220	8.5

To obtain the highest strength, the heat treatment parameters should be optimized from the standpoint of maximum precipitation hardening and contribution of grain-boundary hardening. The results obtained were used to determine the optimum mode for solution treatment, i.e., 500°C, 8 h.

Figure 7 presents the microstructure (SEM) of alloy Mg − 10Gd − 3Y − 0.6Zr after the T4 treatment (520°C, 8 h), which illustrates the presence of cuboid particles, and the results of the point EDS analysis. The cuboid particles 1 − 4 μm in size are arranged primarily over grain boundaries. According to the data of the energy dispersive spectroscopy, these

particles contain an elevated amount of Gd and Y (over 50% in total). This agrees with the data of [9], where the cuboid phase is shown to have a fcc crystal lattice with constant 560 pm.

Figure 8 presents the variation of the hardness of the alloy as a function of the time of aging at 220°C after the 8-h solution treatment at 500°C. The peak of the hardness (126 *HV*) is observed after about 16 h of aging, which is followed by overaging. The authors of [8, 9] give the following succession of decomposition of the solid solution in an alloy of the Mg-Y-REM system: supersaturated solid solution (S.S.S.S.) $\rightarrow \beta''$ (D0$_{19}$) $\rightarrow \beta'$ (orthorhombic body-centered) $\rightarrow \beta_1$ (fcc) $\rightarrow \beta$ (fcc). In the early stages of the aging the structure contains spherical precipitates of phase β'', and the hardness is low. Formation of precipitates of phase β' causes growth of the hardness to a maximum value, when only this
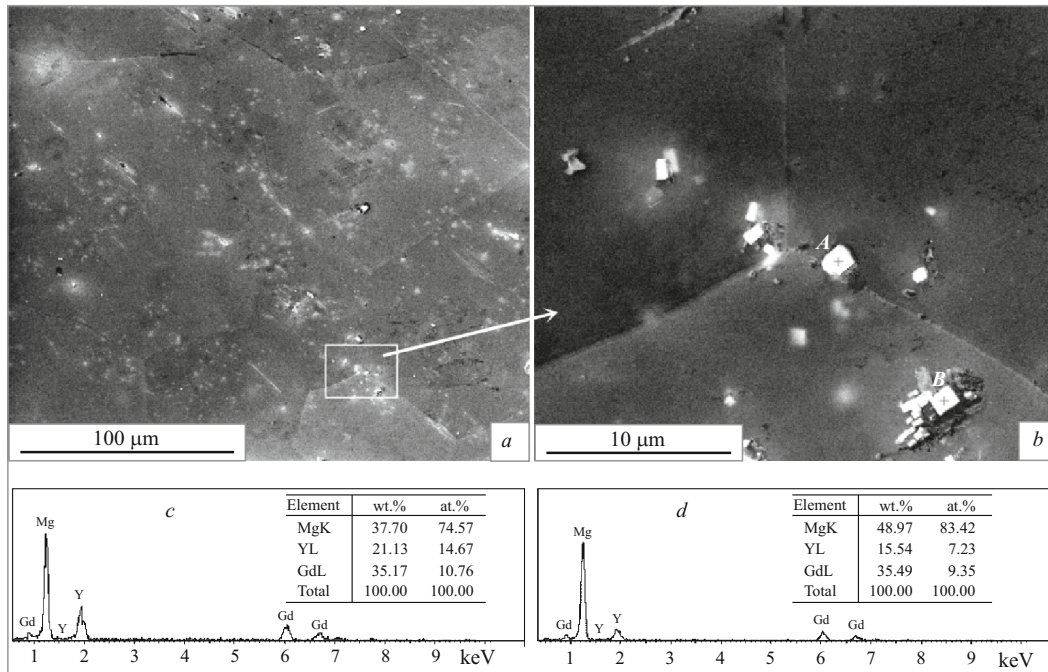

Fig. 7. Microstructure (SEM) of alloy Mg − 10Gd − 3Y − 0.6Zr after casting and T4 treatment (520°C, 8 h) (*a*), a magnified image of cuboid phases (*b*), and energy dispersive spectroscopy at points *A* (*c*) and *B* (*d*).
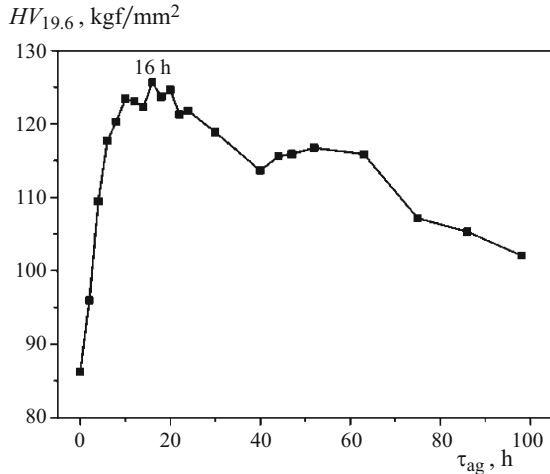
$HV_{19.6}$, kgf/mm^2

Fig. 8. Hardness of alloy Mg – 10Gd – 3Y – 0.6Zr after the T4 treatment (520°C, 8 h) as a function of the duration of aging at 220°C.

TABLE 2. Mechanical Properties of Alloy Mg – 10Gd – 3Y – 0.6Zr (Tensile Tests) after Solution Treatment and Aging at 220°C for 16 h (Maximum Hardness)

Treatment mode T4	$\sigma_{0.2}$, MPa	σ_r , MPa	δ, %
480°C, 5 h	198	318	6.3
480°C, 8 h	199	322	5.8
500°C, 5 h	201	334	6.6
500°C, 8 h	208	346	7.4
520°C, 5 h	205	341	6.9
520°C, 8 h	201	334	6.3

kind of precipitates is present. In the stage of overaging the precipitates of phase β_1 become dominant and are then replaced by an equilibrium β-phase; the hardness decreases rapidly.

Table 2 presents the mechanical properties of alloy Mg – 10Gd – 3Y – 0.6Zr after a solution treatment and 16-h aging at 220°C. It can be seen that as compared to the as-cast condition the yield strength increases by only 11 – 22 MPa, and the ultimate strength increases by 92 – 120 MPa. The strength has a maximum value of 346 MPa after the T6 treatment and is equal to 225 MPa after the T4 treatment. According to the data of [10], the main reason behind the growth in the strength is precipitation of particles of phase β'.

Figure 9 presents fracture surfaces of specimens of alloy Mg – 10Gd – 3Y – 0.6Zr in different states after tensile tests. In the cast condition we can observe dimples, tearing ridges and a few cleavage planes (Fig. 9a). After the 8-h solution treatment at 500°C, we observe primarily cleavage planes and evident river patterns (Fig. 9b) as compared to the cast condition. The eutectic phases have dissolved, the cleavage planes have come wider, and the river patterns with small steps have become more manifested. After the T6 treatment, the fracture surface is chiefly represented by cleavage planes and observable grain boundaries due to the phases precipitated on them (Fig. 9c). This indicates that the kind of the tensile fracture has changed from a combination of transgranular and dimple fracture to intergranular fracture under the T6 treatment.

CONCLUSIONS

1. The microstructure of alloy Mg – 10Gd – 3Y – 0.6Zr in cast condition is represented by a magnesium-base α-solid solution and a $Mg_{24}(Gd, Y)_5$ eutectic phase. During the solution treatment, this phase dissolves in the matrix virtually completely; the matrix in this condition contains cuboid particles of a phase enriched with gadolinium and yttrium.

2. In the process of aging, the hardness varies over a curve with a maximum (126 HV) at a hold for 16 h. The treatment optimum from the standpoint of mechanical strength consists of 8-h solution treatment at 500°C and 16-h aging at 220°C. The ultimate tensile strength in this condition is 346 MPa at an elongation of 7.4%.

3. The type of fracture under tension varies from a combination of transgranular and dimple fracture after the solution treatment to intergranular fracture after the T6 treatment.
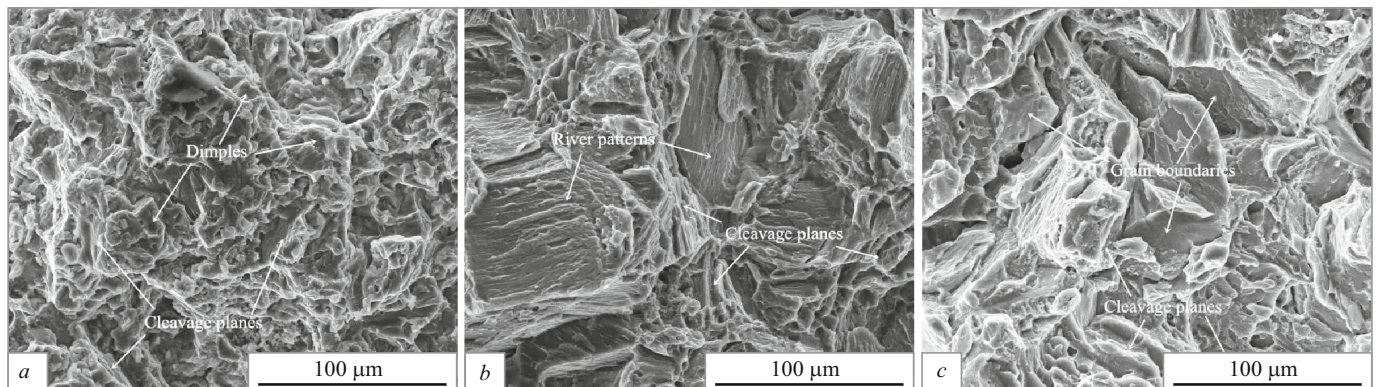

Fig. 9. Fracture surfaces (SEM) of specimens of alloy Mg – 10Gd – 3Y – 0.6Zr tested for tensile strength in different conditions: *a*) as cast; *b*) T4 treatment (500°C, 8 h); *c*) T6 treatment (220°C, 16 h).

REFERENCES

1. W. C. Liu, L. K. Jiang, L. Cao, et al., "Fatigue behavior and plain-strain fracture toughness of sand-cast Mg – 10Gd – 3Y – 0.5Zr magnesium alloy," *Mater. Des.*, **59**, 466 – 474 (2014).

2. L. Zheng, C. M. Liu, Y. C. Wan, et al., "Microstructures and mechanical properties of Mg – 10Gd – 6Y – 2Zn – 0.6Zr (wt.%) alloy," *J. Alloys Compd.*, **509**, 8832 – 8839 (2011).

3. C. Xu, M. Y. Zheng, S. W. Xu, et al., "Ultra high-strength Mg – Gd – Y – Zn – Zr alloy sheets processed by large-strain hot rolling and ageing," *Mater. Sci. Eng. A*, 547, 93 – 98 (2012).

4. A. A. Luo, "Recent magnesium alloy development for elevated temperature applications," *J. Mater. Sci.*, **1**, 2 – 22 (2013).

5. A. Luo, "Cast magnesium alloys for elevated temperature applications," *J. Mater. Sci.*, **49**, 13 – 30 (2004).

6. C. Suman, *SAE Technical Paper 910416*, Soc. Automotive Engineers, Warrendale, PA (1991).

7. J. Wang, J. Meng, D. P. Zhang, and D. X. Tang, "Effect of Y for enhanced age hardening response and mechanical properties of Mg – Ho – Y – Zr alloys," *Mater. Sci. Eng. A*, **456**, 78 – 84 (2007).

8. H. R. Jafari Nodooshan, W. C. Liu, G. H. Wu, et al., "Microstructure characterization and high-temperature shear strength of the Mg – 10D – 3Y – 1.2Zn – 0.5Zr alloy in the as-cast and aged conditions," *J. Alloys Compd.*, **619**, 826 – 833 (2015).

9. S. M. He, X. Q. Zeng, L. M. Peng, et al., *J. Alloys Compd.*, **421**, 309 – 313 (2006).

10. S. M. He, X. Q. Zeng, L. M. Peng, et al., "Precipitation in a Mg – 10Gd – 3Y – 0.4Zr (wt.%) alloy during isothermal ageing at 250°C," *J. Alloys Compd.*, **427**, 316 – 323 (2007).

11. M. Sun, G. H. Wu, W. Wang, and W. J. Ding, "Effect of Zr on the microstructure, mechanical properties and corrosion resistance of Mg – 10Gd – 3Y magnesium alloy," *Mater. Sci. Eng. A*., **523**, 145 – 151 (2009).

12. J. W. Chang, X. W. Guo, S. M. He, et al., "Investigation of the corrosion for Mg – xGd – 3Y – 0.4Zr (x = 6, 8, 10, 12 wt.%) alloys in a peak-aged condition," *Corros. Sci.*, **50**, 166 – 177 (2008).

13. H. R. Jafari Nodooshan, W. C. Liu, G. H. Wu, et al., "Effect of Gd content on microstructure and mechanical properties of Mg – Gd – Y – Zr alloys under peak-aged condition," *Mater. Sci. Eng. A*, **615**, 79 – 86 (2014).

14. L. Huo, Z. Q. Han, and B. C. Liu, "Effect of microstructure on tensile and fatigue properties of cast Mg – 10Gd – 2Y – 0.5Zr alloy," *Int. J. Cast Met. Res.*, **22**, 123 – 126 (2009).

15. T. Honma, T. Ohkubo, K. Hono, and S. Kamado, "Chemistry of nanoscale precipitates in Mg – 2.1Gd – 0.6Y – 0.2Zr (at.%) alloy investigated by the atom probe technique," *Mater. Sci. Eng. A*, **395**, 301 – 306 (2005).

16. F. Yang, F. Lv, X. M. Yang, et al., "Enhanced very high cycle fatigue performance of extruded Mg – 12Gd – 3Y – 0.5Zr magnesium alloy," *Mater. Sci. Eng. A*, **528**, 2231 – 2238 (2011).